Studies on Thermoplastic Polyurethanes Based on New Diphenylethane-Derivative Diols. III. The Effect of Molecular Weight and Structure of Soft Segment on Some Properties of Segmented Polyurethanes

Magdalena Rogulska,[1] Anna Kultys,[1] Stanisław Pikus[2]

[1]*Department of Polymer Chemistry, Faculty of Chemistry, Maria Curie-Skłodowska University, ul. Gliniana 33, 20-614 Lublin, Poland*
[2]*Department of Crystallography, Faculty of Chemistry, Maria Curie-Skłodowska University, Pl. Marii Curie-Skłodowskiej 3, 20-031 Lublin, Poland*

Received 5 November 2007; accepted 31 March 2008
DOI 10.1002/app.28583
Published online 28 July 2008 in Wiley InterScience (www.interscience.wiley.com).

ABSTRACT: Two series of poly(ether urethane)s and one series of poly(ester urethane)s were synthesized, containing, respectively, poly(oxytetramethylene) diol (PTMO) of $\overline{M}_n$ = 1000 and 2000 and poly(ε-caprolactone) diol of $\overline{M}_n$ = 2000 as soft segments. In each series the same hard segment, i.e., 4,4′-(ethane-1,2-diyl)bis(benzenethiohexanol)/hexane-1,6-diyl diisocyanate, with different content (∼ 14–72 wt %) was used. The polymers were prepared by a one-step melt polymerization in the presence of dibutyltin dilaurate as a catalyst, at the molar ratio of NCO/OH = 1 (in the case of the polymers from PTMO of $\overline{M}_n$ = 1000 also at 1.05). For all polymers structures (by FTIR and X-ray diffraction analysis) and physicochemical, thermal (by differential scanning calorimetry and thermogravimetric analysis), and tensile properties as well as Shore A/D hardness were determined. The resulting polymers were thermoplastic materials with partially crystalline structures (except the polymer with the highest content of PTMO of $\overline{M}_n$ = 2000). It was found that the poly(ether urethane)s showed lower crystallinity, glass-transition temperature (T_g), and hardness as well as better thermal stability than the poly(ester urethane)s. Poly(ether urethane)s also exhibited higher tensile strength (up to 23.5 MPa vs. 20.3 MPa) and elongation at break (up to ∼ 1950% vs. 1200%) in comparison with the corresponding poly(ester urethane)s. Among the poly(ether urethane)s an increase in soft-segment length was accompanied by an increase in thermal stability, tensile strength, and elongation at break, as well as a decrease in T_g, crystallinity, and hardness.
 J Appl Polym Sci 110: 1677–1689, 2008

Key words: thermoplastic polyurethane elastomers (TPUs); sulfur-containing aliphatic–aromatic α,ω-diols; hexane-1,6-diyl diisocyanate (HDI); poly(oxytetramethylene) diol (PTMO); poly(ε-caprolactone) diol (PCL); thermal and mechanical properties

INTRODUCTION

Thermoplastic polyurethane elastomers (TPUs) offer mechanical properties that are characteristics of rubbers (softness, flexibility, and resilience) but can be processed by methods used for thermoplastic materials (because of the absence of chemical networks, which normally exist in rubbers). It can be said that they form a bridge between conventional rubbers and thermoplastics. TPUs possess the unique property of combining high strength, hardness, and modulus together with high elongation at break. They also show excellent abrasion and tear properties as well as excellent resistance to most types of aliphatic and aromatic fluids.[1–4]

The interesting and versatile properties of TPUs are, in part, caused by their segmented structure. TPUs are block copolymers with an alternating sequence of hard and soft segments. The hard segments, composed of diisocyanates and short-chain diols, particularly affect the modulus, hardness, and tear strength. The soft segments, formed by long-chain diols, control flexibility, softness, and low-temperature resistance.[1–6]

The properties of TPUs are greatly influenced in many factors, e.g., the chemical type of components forming hard and soft segments, molecular weight of hard and soft segments, as well as the ratio of these hard and soft block components.[1,2,5]

The most commonly used soft segments are polyether diols [e.g., poly(oxytetramethylene) diol (PTMO), poly(oxyethylene) diol, and poly(oxypropylene) diol] and polyester diols [e.g., poly(ε-caprolactone) diol

Correspondence to: M. Rogulska (magdalena.rogulska@umcs.lublin.pl).
Contract grant sponsor: Polish Committee for Scientific Research; contract grant number: 4T09B 109 23.

TABLE I
Characteristic of Materials Used for the Synthesis of the PURs

Material (designation)	Structure	Supplier
Diisocyanate		
Hexane-1,6-diyl diisocyanate (HDI)	$OCN-(CH_2)_6-NCO$	Fluka
Polyols		
Poly(oxytetramethylene) diol of $\overline{M}_n$ = 1,000 (PTMO-1000)	$H-[O-(CH_2)_4]_m-OH$	BASF
Poly(oxytetramethylene) diol of $\overline{M}_n$ = 2,000 (PTMO-2000)		Aldrich Chemical Company
Poly(ε-caprolactone) diol of $\overline{M}_n$ = 2,000 (PCL-2000)	$H-[O-(CH_2)_5-C(=O)]_m-OH$	Aldrich Chemical Company
Chain extender		
4,4′-(Ethane-1,2-diyl)bis(benzenethiohexanol) (EBTH)	$HO-(CH_2)_6-S-C_6H_4-CH_2-CH_2-C_6H_4-S-(CH_2)_6-OH$	
Catalyst		
Dibutyltin dilaurate (DBTDL)	$[CH_3(CH_2)_3]_2Sn[OCO(CH_2)_{10}CH_3]_2$	Merck-Schuchardt

(PCL), poly(ethylene adipate) diol, and poly(butylene adipate) diol)] with typical molecular weight that ranges from 1000 to 3000.[1–3] The influence of the kind and/or length of both types of soft segments on the morphology and various properties of TPUs has been presented in many articles. Most of these studies concern TPUs based on aliphatic chain extenders, mainly butane-1,4-diol and aromatic diisocyanates, mainly 4,4′-diphenylmethane diisocyanate.[6–44]

In general, the TPUs with the polyester soft segments show higher tensile strength, hardness, and modulus of elasticity as well as smaller extensibility in comparison with the TPUs with the polyether soft segments.[2] Moreover, the polyester TPUs also exhibit better oxidation stability, but worse hydrolytic resistance when compared with the polyether TPUs.[5–8]

The purpose of our investigations was to synthesize three series of novel segmented polyurethanes (PURs) based on aliphatic diisocyanate, and to study the effect of the kind and molecular weight of the soft segment used on crystallinity and some physicochemical, thermal, and mechanical properties of the resulting polymers. The PURs were prepared from 20 to 80 mol % PTMO of $\overline{M}_n$ = 1000 or 2000 (PTMO-1000 or PTMO-2000) or PCL of $\overline{M}_n$ = 2000 (PCL-2000) as soft segments, hexane-1,6-diyl diisocyanate (HDI) and 4,4′-(ethane-1,2-diyl)bis(benzenethiohexanol) (EBTH) as a nonconventional chain extender.

EXPERIMENTAL

Materials

The products employed in this study are listed in Table I.

EBTH (mp = 116–117°C, M = 446.7) was obtained in our laboratory and its synthesis was described previously.[45] Other reagents such as HDI (>99%) and DBTDL were used as received. Before being used, PTMO and PCL were heated at 120°C *in vacuo* for 2 h.

Characterization techniques

Reduced viscosity

Reduced viscosities (η_{red}s, dL/g) of 0.5% polymer solution in the phenol/1,1,2,2-tetrachloroethane (Ph/TChE) mixture with a weight ratio of 1 : 3 were measured in an Ubbelohde viscometer (Gliwice, Poland) at 25°C.

Gel permeation chromatography

The number ($\overline{M}_n$) and weight ($\overline{M}_w$) average molecular weights, and the index of the molecular weight distribution ($\overline{M}_w/\overline{M}_n$) for some PURs were done on a Knauer instrument at 30°C. Tetrahydrofuran (THF) was used as an eluent (flow rate = 1 mL/min). The system was equipped with a set of five PL-gel columns (10 μm) with a refractive-index detector and

was calibrated against narrow molecular weight polystyrene standards.

Fourier transform infrared spectroscopy

The FTIR measurements were made using a Perkin–Elmer 1725 X FTIR spectrophotometer. Thin films or KBr discs were employed.

X-ray diffraction analysis

The XRD analysis was performed with a DRON-3 X-ray apparatus (St. Petersburg, Russia) with a copper tube and nickel filter. The XRD patterns of investigated samples were obtained via the measurement of the number of impulses within a given angle over 10 s. The measurements were taken for every 0.02° at 22°C. The XRD patterns were analyzed by WAXSFIT computer program.[46] The program resolves a diffraction curve on diffraction peaks and amorphous halo, which allows estimating the crystallinity degree.

Thermogravimetric analysis

The thermal stabilities of the PURs were examined using a MOM 3427 derivatograph (Paulik, Paulik and Erdey; Budapest, Hungary) at the heating rate of 10°C/min in air, in the range of 20–1000°C; measurement relative to Al_2O_3.

Differential scanning calorimetry

The DSC thermograms were obtained using a NETZSCH 204 calorimeter over the temperature range −100 to 200°C. The reported transitions were taken from first and second heating scans at the heating/cooling rate of 10°C/min. Sample weights about 10–15 mg were used. Glass-transition temperatures (T_gs) for the polymer samples were taken as an inflection point on curves of heat-capacity changes. Melting temperatures (T_ms) for the polymer samples were read at endothermic-peak maxima.

Hardness

Polyurethane hardness was measured by the Shore A/D method on a Zwick 7206/H04 hardness tester at 23°C. The values were taken after 15 s.

Tensile properties

Stress–strain behavior was determined by a TIRA Test 2200 tensile-testing machine according to Polish Standard PN-81/C-89034 (EN ISO Standard 527-1 : 1996, 527-2 : 1996). The measurements were performed at 23°C at the speed of 100 mm/min. The tensile test pieces, 1-mm thick and 6-mm wide (for the section measured), were cut from the pressed sheet.

Synthesis of the PURs

All the PURs were synthesized by a one-step melt polymerization using 20, 40, 50, 60, and 80 mol % PTMO or PCL, EBTH, and HDI. The reaction was conducted at 1 : 1*M* ratio of dihydroxyl compounds to diisocyanate, and in the case of the polymers from PTMO-1000 also at 1 : 1.05. DBTDL was used as a catalyst.

The general procedure for the synthesis of the PURs by this method was as follows: PTMO or PCL and EBTH (0.01 mol together), and HDI (0.01 or 0.0105 mol) were heated with stirring under dry nitrogen to 120°C (an oil bath). A catalytic amount of DBTDL was added to the clear melt and polymerization rapidly began at vigorous stirring. The reaction temperature was gradually raised to 140°C and the formed colorless, rubber-like or hard product was additionally heated at this temperature for 2 h.

RESULTS AND DISCUSSION

PUR synthesis and characterization

The new HDI-based segmented PURs were synthesized from various soft segments: PTMO-1000, PTMO-2000, or PCL-2000. EBTH was used as a chain extender.

The designations, η_{red} values and GPC data of the PURs are listed in Table II. As can be seen in Table II, the η_{red} values (in the range of 1.14–5.33 dL/g) were determined for all the synthesized PURs (in the Ph/TChE mixture), but molecular weights (by GPC) only for the polymers soluble in THF. On the basis of the obtained data it can be said that the PURs with higher molecular weights were prepared from longer soft segments (PTMO-2000 and PCL-2000) and in the case of the PTMO-1000 based PURs with excess of diisocyanate. The PURs were soluble in TChE, *N*,*N*-dimethylacetamide (except L2-20, P1-20), *N*,*N*-dimethylformamide (except L2-20, P1-20), *N*-methyl-2-pyrrolidone (except L2-20) at room or elevated (80–90°C) temperature and in the Ph/TChE mixture at room temperature. None of the polymers was soluble in dimethyl sulfoxide. Generally, a better solubility was shown by the PURs based on PTMO-2000 than PTMO-1000 and the poly(ether urethane)s than the poly(ester urethane)s. The solubility increased with increasing soft-segment content.

The structures of the PURs studied (at the molar ratio of NCO/OH = 1) were examined by FTIR and XRD analysis.

FTIR spectra of the poly(ether urethane)s indicated the following bands (in cm^{-1}): 1736–1720 (nonbonded

TABLE II
Designations, η_{red} Values and GPC Data of the PURs

PUR	Soft segment	Soft-segment content (mol %)	Hard-segment content[a] (wt %)	η_{red}[b] (dL/g)	GPC data[b,c]		
					$\overline{M}_n$	$\overline{M}_w$	$\overline{M}_w/\overline{M}_n$
P1-20	PTMO-1000	20	72.4	1.29 (3.00)	–	–	–
P1-40		40	52.2	1.52 (5.33)	–	–	–
P1-50		50	43.9	1.14 (3.48)	–	–	–
P1-60		60	36.6	1.33 (3.39)	10,500[d] (16,300[d])	22,100[d] (44,300[d])	2.11[d] (2.71[d])
P1-80		80	24.3	1.46 (1.75)	16,900	34,100	2.01
P2-20	PTMO-2000	20	56.9	1.85	–	–	–
P2-40		40	35.3	2.26	–	–	–
P2-50		50	28.2	2.00	–	–	–
P2-60		60	22.5	2.07	33,700	80,890	2.40
P2-80		80	14.0	2.18	46,440	105,100	2.26
L2-20	PCL-2000	20	56.9	2.02	–	–	–
L2-40		40	35.3	1.69	–	–	–
L2-50		50	28.2	2.17	–	–	–
L2-60		60	22.5	1.92	–	–	–
L2-80		80	14.0	2.58	–	–	–

[a] $\text{Hard}-\text{segment content} = \frac{\text{HDI} + \text{EBTH (weight)}}{\text{PTMO}-1000/\text{PTMO}-2000/\text{PCL}-2000 + \text{HDI} + \text{EBTH (weight)}}$.
[b] Data in parentheses are values for the PURs obtained at the molar ratio of NCO/OH = 1.05.
[c] GPC measurements were performed for the PURs soluble in THF.
[d] GPC data of the soluble fraction.

C=O stretching of the urethane group); 1708–1682 (bonded C=O stretching of the urethane group); 3402–3323 (N—H stretching) and 1538–1535 (N—H bending) of the urethane group; 1115–1109 (C—O stretching of the ether group); 2942–2926 and 2858–2855 (asymmetric and symmetric C—H stretching of CH_2, respectively).

FTIR spectra of the poly(ester urethane)s showed the following bands (in cm^{-1}): 1741–1731 (non-bonded C=O stretching of the urethane and ester groups); 1687–1685 (bonded C=O stretching of the urethane and ester groups); 3332–3329 (N—H stretching) and 1538–1530 (N—H bending) of the urethane group; 1169–1167 (C—O stretching of the ester group); 2942–2932 and 2864–2859 (asymmetric and symmetric C—H stretching of CH_2, respectively).

Figure 1 presents the typical FTIR spectra of the chosen PURs.

Thermal properties

TGA and DSC were done for all the PURs obtained at the molar ratio of NCO/OH = 1, and the numerical data are summarized in Tables III and IV, respectively. The DSC curves of the polymers based on PTMO-1000, PTMO-2000, and PCL-2000 are presented in Figures 2–4, respectively, whereas Figure 5 additionally shows the DSC curves of the hard-segment-type and soft-segment-type polymers.

TGA

A better thermal stability (higher T_i, T_5, T_{10}, and T_{50}) was shown by the poly(ether urethane)s. Among the poly(ether urethane)s, generally, higher T_i, T_5, and T_{10} but lower T_{50} and T_{max} were exhibited by the polymers with the longer soft segment. A smaller

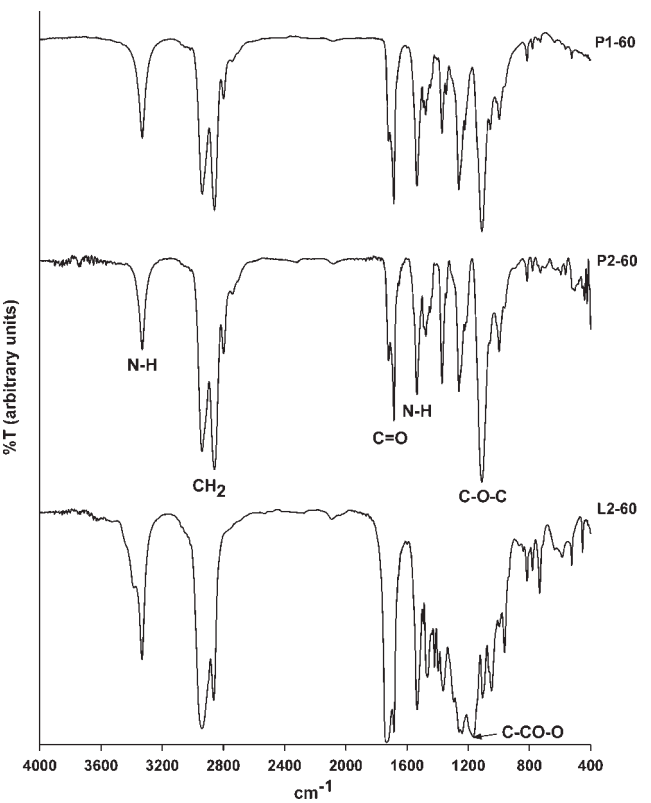

Figure 1 FTIR spectra of the PURs.

TABLE III
TGA Data of the PURs

PUR	T_i[a] (°C)	T_5[b] (°C)	T_{10}[c] (°C)	T_{50}[d] (°C)	T_{max}[e] (°C)
P1-20	250	315	330	410	415
P1-40	240	315	330	410	410
P1-50	240	315	330	410	410
P1-60	250	310	340	410	410
P1-80	230	310	330	410	410
P2-20	260	320	340	400	405
P2-40	255	320	340	400	400
P2-50	250	320	340	400	400
P2-60	250	320	340	400	405
P2-80	230	310	330	390	400
L2-20	240	300	320	400	415
L2-40	230	295	320	390	420
L2-50	230	290	310	380	385
L2-60	225	280	305	375	375
L2-80	220	285	305	370	380

[a] The temperature of initial decomposition from the thermogravimetric (TG) curve.
[b] The temperature of 5% weight loss from the TG curve, respectively.
[c] The temperature of 10% weight loss from the TG curve, respectively.
[d] The temperature of 50% weight loss from the TG curve, respectively.
[e] The temperature of the maximum rate of weight loss from the minimum of differential TG curve.

influence of soft-segment content on thermal stability was observed for the poly(ether urethane)s than for the poly(ester urethane)s. In the case of the poly(ester urethane)s, an increase in PCL content caused a decrease in T_i, T_5, T_{10}, and T_{50}.

DSC

The DSC curves received for the studied poly(ether urethane)s (Figs. 2 and 3) showed distinct T_gs of the soft segments for the polymers with 40–80 mol % PTMO-1000 content and 20–80 mol % PTMO-2000 content, from first and/or second heating scans, in the range of −73 to −68°C and −75 to −61°C, respectively. The T_g values were the same or similar to the values received for the pure soft segments (see Fig. 5). This points to a good microphase separation in these polymers. In both heating scans a few endothermic peaks at 4–151°C were observed. The lower-temperature peaks at 4–45°C were associated with the soft-segment melting (see Fig. 5). The soft-segment melting endotherms with lower T_m (below room temperature) were seen for the PURs with PTMO-2000. These polymers were also characterized by a higher ability to crystallize the soft segment (on the basis of the presence of the distinct soft-segment melting endotherms on all DSC curves and the higher heat of fusion (ΔH) values in comparison with the PTMO-1000 based PURs. The endothermic peaks at 51–151°C were probably connected with the hard-segment melting (see Fig. 5). The peaks at lower temperatures correspond to the melting of less (short-range) ordered structures, but those at higher temperatures to greater (long-range) ordered structures.

TABLE IV
DSC Data of the PURs

	Soft segment						Hard segment			
	T_g (°C)		T_m (°C)		ΔH (J/g)		T_m (°C)		ΔH (J/g)	
PUR	I[a]	II[a]	I[a]	II[a]	I[a]	II[a]	I[a]	II[a]	I[a]	II[a]
P1-20	–[b]	–[b]	–[c]	–[c]	–[c]	–[c]	56, 113, 146	114, 144	1.7, 35.4	35.5[d]
P1-40	–[b]	−68	–[c]	–[c]	–[c]	–[c]	53, 105, 135	100, 133	0.7, 45.2[d]	46.2[d]
P1-50	–[b]	−68	–[c]	–[c]	–[c]	–[c]	51, 103, 130	99, 127	1.8, 31.9[d]	44.9[d]
P1-60	–[b]	−71	45	23	3.0	1.1	123	90, 120	15.9	31.3[d]
P1-80	–[b]	−73	42	32	8.5	6.1	101	100	12.0	9.6
P2-20	−71	−61	6	5	9.6	7.3	56, 105, 151	110, 144	47.3[d]	41.2[d]
P2-40	−74	−73	4	4	12.6	10.9	60, 112, 128, 140, 147	109, 131	34.8[d]	33.0[d]
P2-50	–[b]	−73	9	10	23.6	18.4	58, 113, 131	112, 126	30.9[d]	29.0[d]
P2-60	−74	−75	12	12	23.4	24.6	59, 114	109	29.7[d]	18.8
P2-80	−74	−75	17	24	37.9	46.4	63, 94	93	21.0[d]	7.5
L2-20	−52	−52	–[c]	–[c]	–[c]	–[c]	144	104, 140	48.0	43.1[d]
L2-40	−53	−53	43	31	6.1	19.3	129	84, 124	23.1	29.1[d]
L2-50	−53	−53	45	36	14.9	20.5	111, 122	76, 118	18.8[d]	22.9[d]
L2-60	−52	−53	49	40	29.4	30.5	105	69, 102	27.6	12.6[d]
L2-80	−53	−54	53	43	52.0	48.4	87	84	7.4	7.7

[a] I and II—first and second heating scans, respectively.
[b] Too difficult to determine T_g from the thermogram.
[c] Transition not observed.
[d] Total ΔH.

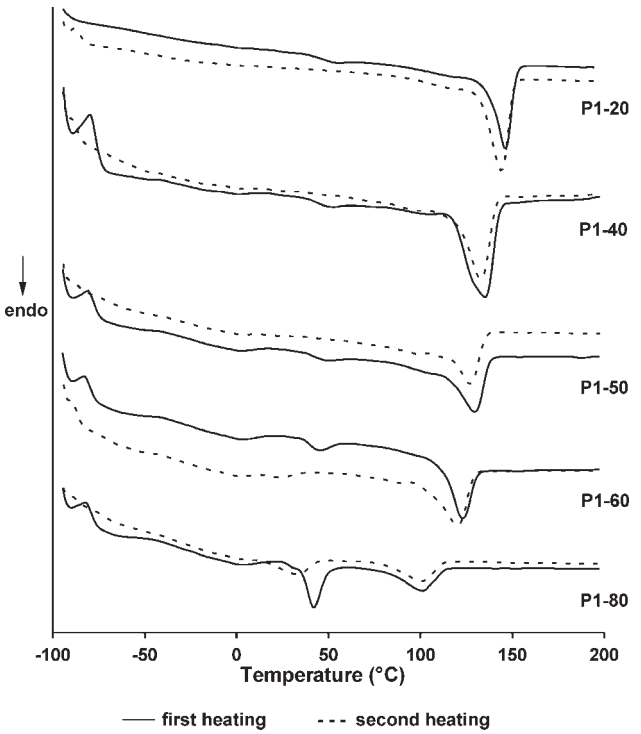

Figure 2 DSC curves of the PURs based on PTMO-1000.

In the case of the polymers with a higher contents of hard segments, one cannot unequivocally interpret the peaks at ~ 50°C, because in this area endothermic effects connected with both the soft and hard segment co-occur (see Fig. 5).

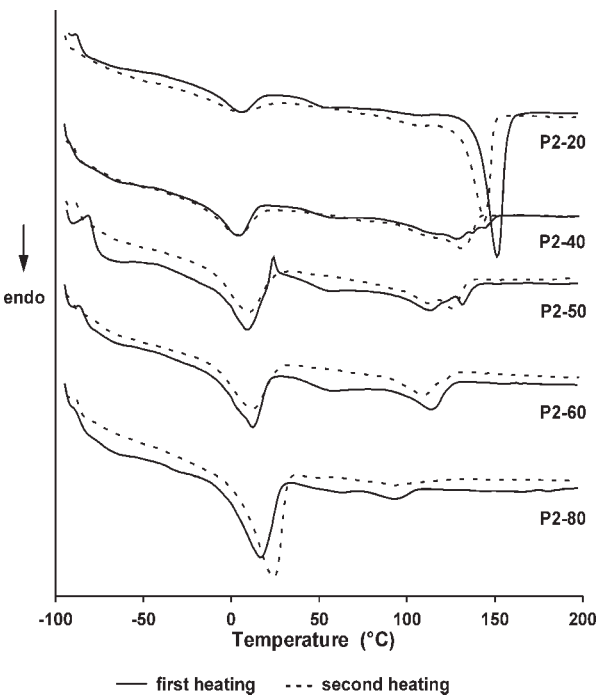

Figure 3 DSC curves of the PURs based on PTMO-2000.

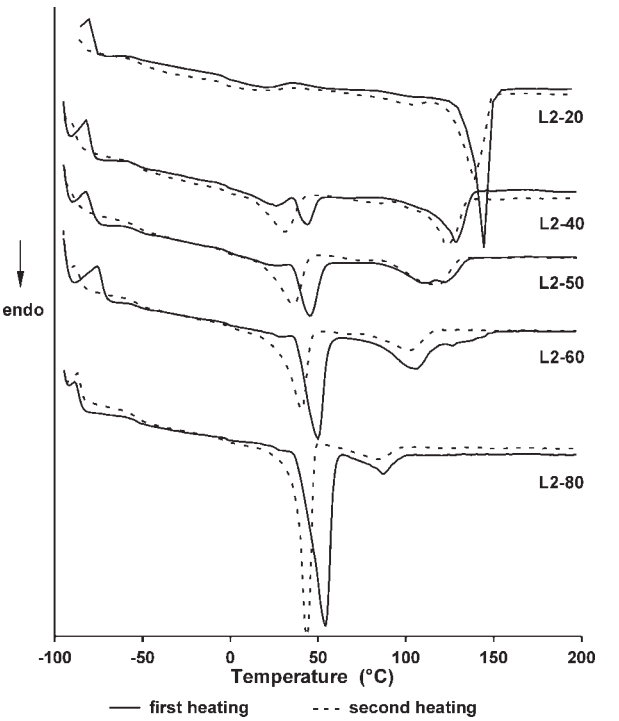

Figure 4 DSC curves of the PURs based on PCL-2000.

The DSC curves of the PCL-2000 based PURs (Fig. 4) exhibited the endothermic peaks of the hard-segment melting at 87–144°C with ΔH ≈7–48 J/g (first heating scans) and 84–140°C with ΔH ≈8–43 J/g

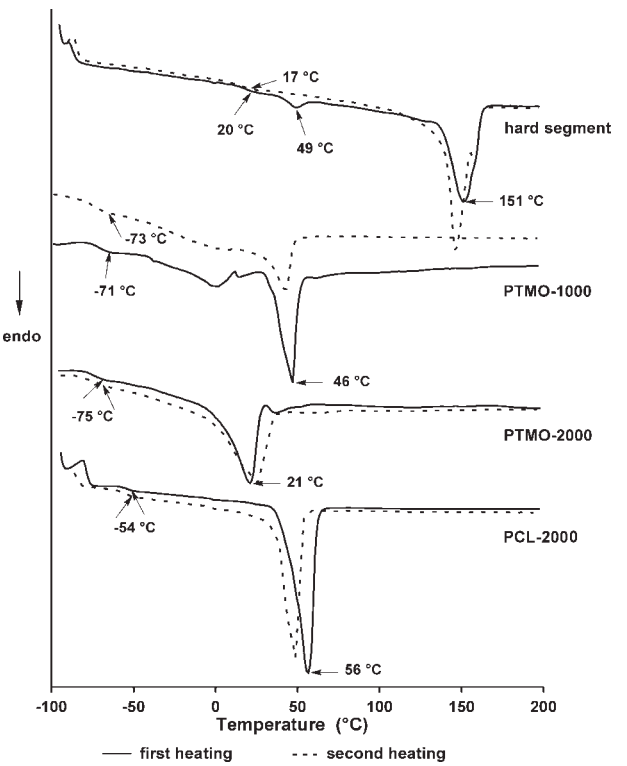

Figure 5 DSC curves of the hard-segment-type and soft-segment-type PURs.

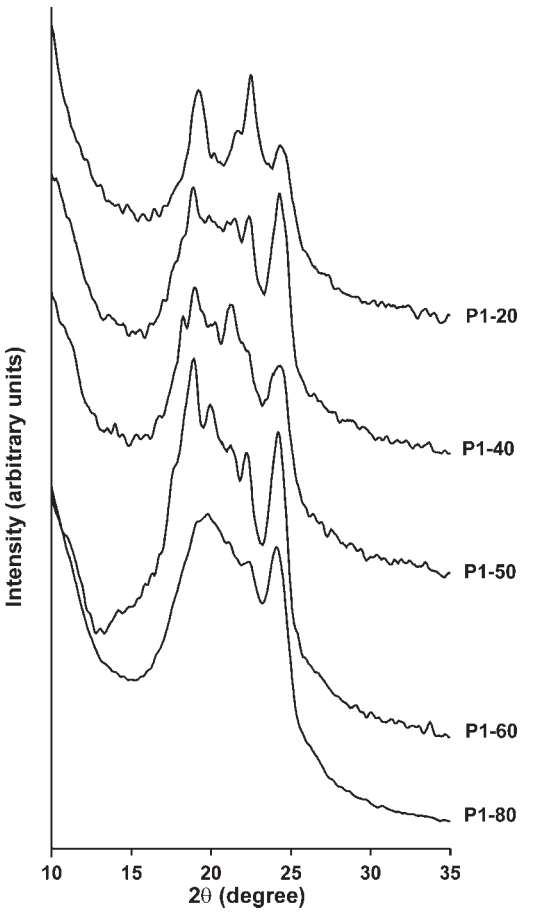

Figure 6 XRD patterns of the PURs based on PTMO-1000.

(second heating scans). For the polymer L2-20 high and sharp endothermic peaks can be observed, which suggests considerable ordering in hard-segment domains. With the increase of PCL-2000 content, a widening of endotherms and a shifting of the maxima of these endotherms to lower temperatures can be seen. It points to a decrease in the ordering of the hard-segment domains in these polymers. In both heating scans endothermic peaks of the soft-segment melting were also observed (except polymer L2-20). It could also be noticed that an increase in soft-segment content caused an increase in the T_m and ΔH values of the soft-segment melting, from 31 to 53°C and from about 6 J/g to about 52 J/g, respectively. On the basis of the ΔH values obtained, it can be said that all this series of polymers was characterized by a high degree of crystallinity, whereas in the range of 20 to 80 mol % PCL-2000 the crystallinity connected with hard segments decreased, and the one connected with soft segments increased. The soft-segment T_gs in the range of −54 to −52°C indicate a good microphase separation in all these PURs (the T_g for the pure PCL-2000 equals −54°C, see Fig. 5).

Generally, in each series of the polymers with the increased soft-segment content the T_m and ΔH of the hard segments decreased, the T_m (for the PTMO-2000 and PCL-2000 series) and ΔH of the soft segments increased, and the soft-segment T_g (in the second heating scans) decreased. Significantly, lower T_gs, i.e., −75 to −61°C vs. −54 to −52°C, were seen for the poly(ether urethane)s. A better microphase separation was shown by the poly(ether urethane)s with a longer soft segment.

XRD analysis

The XRD patterns obtained for the investigated samples of the PURs based on PTMO-1000, PTMO-2000, and PCL-2000 are shown in Figures 6–8, respectively. It can be seen that both the shape of diffraction spectrum and the crystallinity degree of the PUR samples are dependent on the kind and content of the soft segment. The results of the analysis of the XRD patterns by the WAXSFIT program are presented in Tables V–VIII, and on sample plots in Figures 9–11.

As is evident from the data presented in Table VII, for the polymers with the low PCL-2000 content

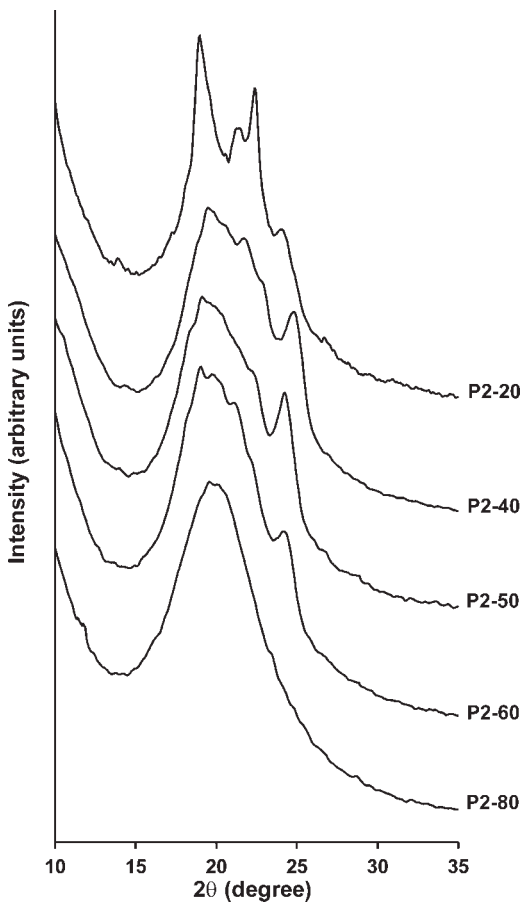

Figure 7 XRD patterns of the PURs based on PTMO-2000.

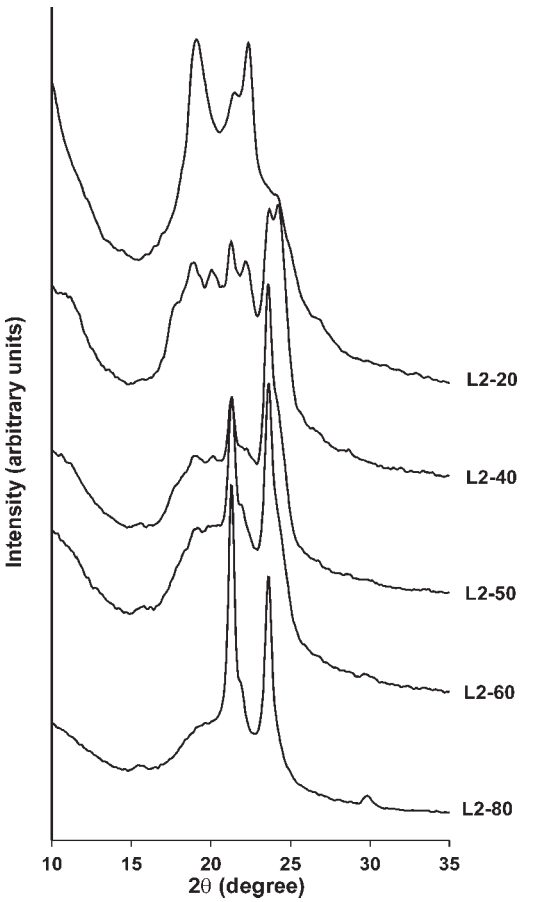

Figure 8 XRD patterns of the PURs based on PCL-2000.

(L2-20, L2-40, and L2-50), apart from the wide amorphous peak (FWHM = 5.3°–6.0°), there are also less wide ones with FWHM in the range of 2.0°–3.3°, which are also included in amorphous peaks. The presence of these peaks next to the relatively sharp diffraction peaks (FWHM = 0.5°–1.0°), indicates the existence in the polymer samples of two phases (except the fully amorphous one), the former is very well-ordered and can be referred to the PCL-2000 soft segment, and the latter is much less well-ordered and corresponds to the hard segment. The increase in the PCL-2000 content in the polymer samples above 50 mol % results in the occurrence on the XRD patterns of very high and narrow diffraction peaks, beside the one wide peak which originates from amorphous areas. This means that in samples L2-60 and L2-80 there exist two phases, the well-crystallized one (the peaks with FWHM <1°) and the fully amorphous one (the peaks with FWHM ~ 6°). The results obtained by DSC and XRD methods for these polymers show a rather good correlation. The presence of high and sharp endothermic peaks on the DSC curves from the first heating scans (see Fig. 4) points to the high crystallinity degree of these PURs. This was confirmed by the XRD patterns obtained (see Figs. 8 and 11, and

TABLE V
XRD Data of the PURs Based on PTMO-1000

PUR	2θ (°)	Full width at half maximum (FWHM) (°)	Height of diffraction peak (a.u.)	Area of diffraction peak (a.u.)
P1-20	19.1[a]	1.2	100	32
	21.5	0.5	21	2
	21.9[b]	6.2	87	100
	22.5	0.9	92	21
	24.5[a]	1.3	65	16
P1-40	18.8[b]	2.6	61	32
	20.4	0.8	8	1
	21.4	1.0	27	5
	21.4[b]	5.9	83	100
	22.4	0.7	44	7
	24.4[a]	1.1	100	23
P1-50	18.1[a]	1.1	47	12
	19.1	1.0	51	8
	20.0	0.6	17	2
	21.0[b]	6.2	100	100
	21.5[b]	1.9	34	10
	24.3[a]	1.3	67	14
P1-60	18.7[b]	2.3	100	47
	20.1	0.6	28	3
	21.1[a]	1.2	31	6
	21.1[b]	7.8	100	100
	22.3	0.7	45	7
	24.2[a]	1.1	92	15
P1-80	19.2[b]	3.4	60	33
	21.3[b]	6.2	100	100
	21.4	0.7	7	1
	22.5	1.0	26	4
	24.2[a]	1.3	83	18

[a] Partially amorphous halo.
[b] Fully amorphous halo.

TABLE VI
XRD Data of the PURs Based on PTMO-2000

PUR	2θ (°)	Full width at half maximum (FWHM) (°)	Height of diffraction peak (a.u.)	Area of diffraction peak (a.u.)
P2-20	19.0[a]	1.1	92	23
	21.1[b]	6.0	100	100
	21.5	0.7	22	3
	22.4	0.6	59	6
	24.3[a]	1.1	23	4
P2-40	19.1[b]	2.9	53	24
	19.8[a]	1.6	13	3
	21.6[b]	6.3	100	100
	22.0[b]	2.0	24	8
	24.9[a]	1.1	49	8
P2-50	18.8[b]	3.0	45	22
	21.0[b]	6.1	100	100
	24.4	1.0	43	7
P2-60	18.9[b]	3.9	50	30
	19.0[b]	1.9	20	6
	21.0[b]	6.3	100	100
	21.3[b]	1.9	18	6
	24.4	1.0	30	5
P2-80	19.5[b]	3.5	43	23
	20.5[b]	6.7	100	100

[a] Partially amorphous halo.
[b] Fully amorphous halo.

TABLE VII
XRD Data of the PURs Based on PCL-2000

PUR	2θ (°)	Full width at half maximum (FWHM) (°)	Height of diffraction peak (a.u.)	Area of diffraction peak (a.u.)
L2-20	19.1[a]	1.3	100	36
	21.0[b]	5.3	98	100
	21.6	1.0	34	6
	22.4	0.6	66	7
	24.1[b]	3.3	42	26
L2-40	18.6[b]	2.5	54	30
	20.2	0.6	15	2
	21.3	0.6	43	9
	21.7[b]	6.0	74	100
	22.2	0.8	33	7
	23.6	0.6	65	10
	24.3	0.9	100	21
L2-50	18.2[b]	2.0	14	17
	19.7[b]	2.7	19	31
	21.3	0.5	34	12
	21.7[b]	5.7	28	100
	22.0	0.7	14	6
	23.7	1.0	100	93
L2-60	20.8[b]	5.9	65	100
	21.3	0.5	68	10
	23.7	0.9	100	34
L2-80	21.2[b]	6.0	30	100
	21.3	0.4	100	34
	23.6	0.5	73	29
	29.8	0.8	5	3
	40.3	0.6	3	1

[a] Partially amorphous halo.
[b] Fully amorphous halo.

TABLE VIII
Crystallinity Degree of the PURs Calculated from XRD Data

	Crystallinity degree (%)				
PUR type	20	40	50	60	80
P1	40.1	21.4	24.7	17.4	14.7
P2	26.5	7.7	5.7	3.4	0.0
L2	28.0	27.4	42.9	30.5	40.1

20, 40, 50, 60, and 80 indicate the soft-segment content (mol %).

Table VIII). A relationship between the PCL-2000 content in the polymer samples and the XRD and DSC data was also observed. For sample L2-20 the DSC curve shows a narrow endothermic peak at 144°C, and it correlates with the presence of the crystalline structure whose diffraction peak is located at a smaller diffraction angle (2θ ~ 18°–20°). Incorporation of a higher PCL-2000 amount into PUR L2-40 caused the appearance of a distinct endothermic peak at temperature ~ 40°C on the DSC curve and a new peak at 2θ ~ 24° on the XRD curve. Further increase in the PCL-2000 content in the remaining samples (L2-50, L2-60, and L2-80) caused an increase of the endothermic peaks connected with the PCL-2000 melting, as well as a decrease and a shifting (to lower temperatures) of the endothermic peaks

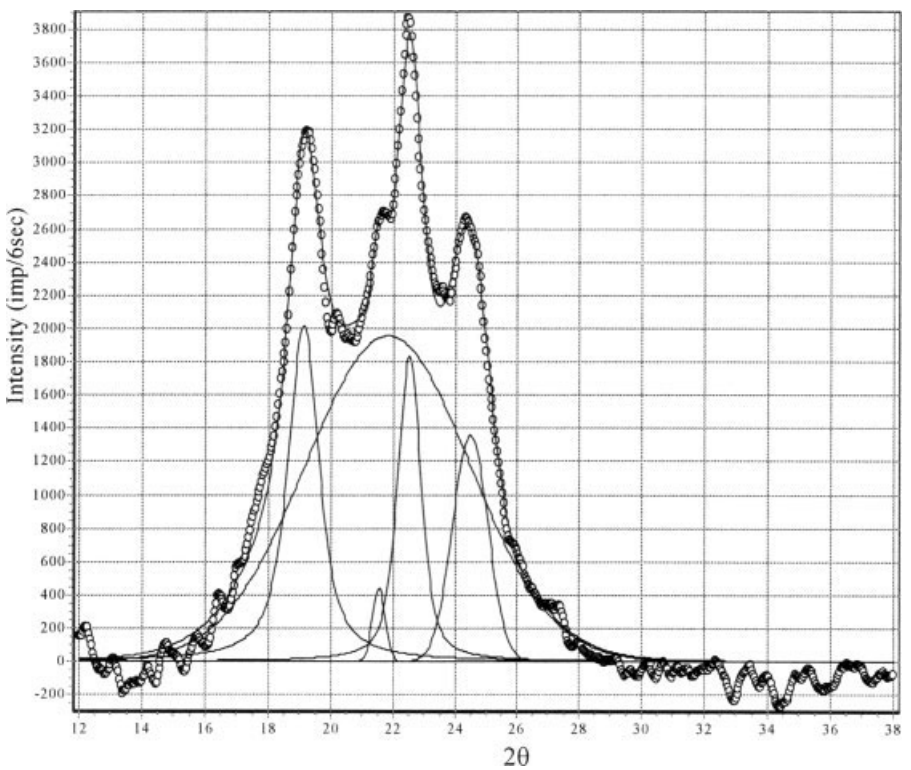

Figure 9 XRD curve (points) of PUR P1-20 resolved into crystalline and amorphous peaks (solid line).

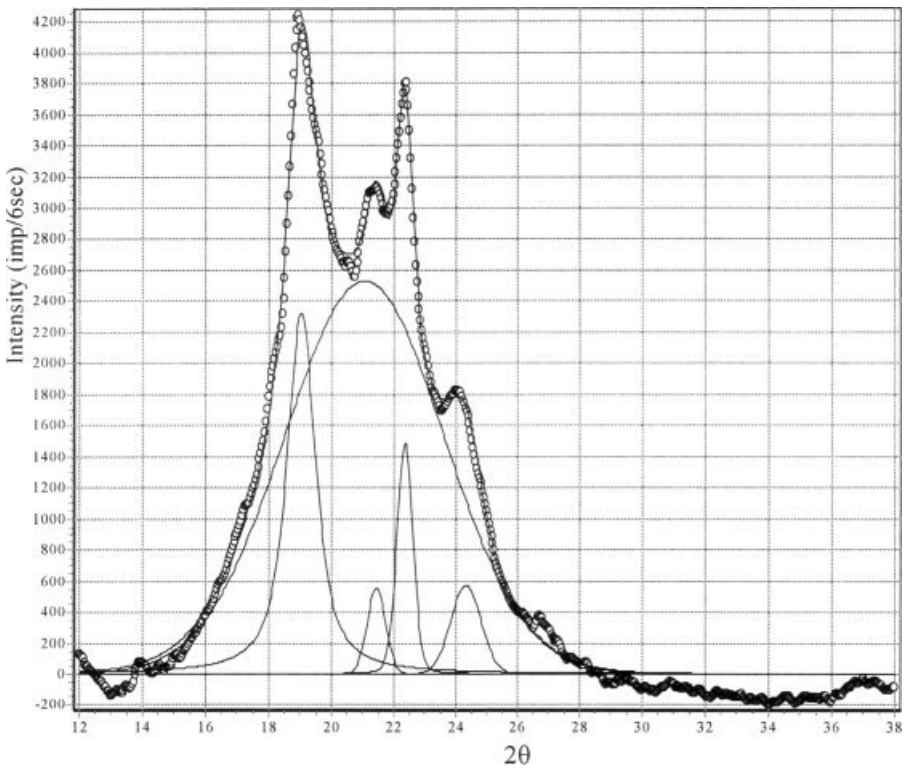

Figure 10 XRD curve (points) of PUR P2-20 resolved into crystalline and amorphous peaks (solid line).

associated with the hard-segment melting on the DSC curves. This was accompanied by an increase of the peaks at $2\theta \sim 21^\circ$ and 24° on the XRD curves.

The PURs derived from PTMO-1000 showed a relatively high crystallinity degree, especially for the polymers with the low PTMO-1000 content (see Figs.

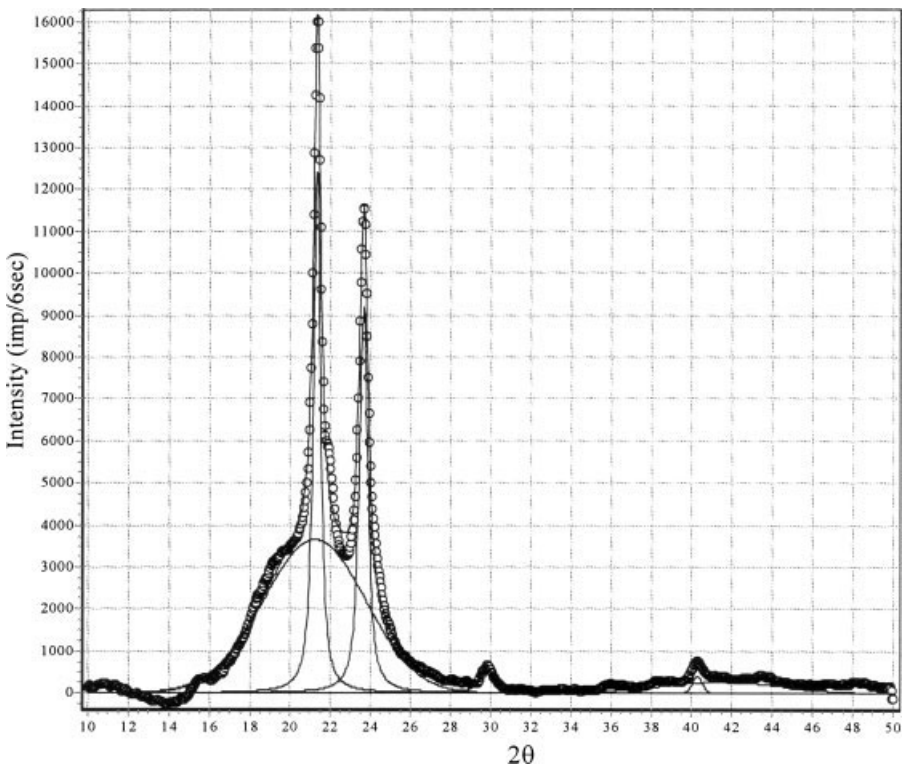

Figure 11 XRD curve (points) of PUR L2-80 resolved into crystalline and amorphous peaks (solid line).

TABLE IX
Hardness and Tensile Properties of the PURs

PUR	Shore hardness		Modulus of elasticity (MPa)	Tensile strength (MPa)	Elongation at break (%)
	A	D			
P1-20[a]	–[b] (95)	–[b] (52)	–[b] (220.2)	–[b] (17.0)	–[b] (17)
P1-40[a]	90 (92)	41 (39)	138.1 (133.1)	15.2 (15.8)	18 (127)
P1-50[a]	89 (90)	34 (35)	130.5 (103.2)	10.9 (13.3)	22 (179)
P1-60[a]	88 (89)	31 (31)	122.7 (90.7)	8.6 (11.7)	26 (235)
P1-80[a]	82 (84)	22 (24)	41.3 (44.5)	6.2 (9.9)	96 (436)
P2-20	92	39	182.6	14.5	57
P2-40	88	29	38.5	22.8	938
P2-50	84	25	34.3	23.5	946
P2-60	76	20	14.1	20.0	1,100
P2-80	57	9	2.3	9.7	1,953
L2-20	94	44	168.0	15.8	155
L2-40	91	34	124.5	13.7	323
L2-50	93	35	120.9	20.3	929
L2-60	93	36	130.0	16.3	1,020
L2-80	94	39	143.7	19.1	1,206

[a] Data in parentheses are values for the PURs obtained at the molar ratio of NCO/OH = 1.05.
[b] The brittle PUR.

6 and 9). With an increase in the soft-segment content in the polymer samples decreased the crystallinity degree, achieving 14.7% for sample P1-80 (see Table VIII). These changes in a polymer structure are partly reflected in the DSC curves from the first heating scans (see Fig. 2). The XRD patterns of the PURs with 20–60 mol % content of PTMO-1000 exhibited distinct peaks, whereas the DSC curves showed fairly distinct endothermic peaks at 123–146°C, disappearing with an increase in the soft-segment content in the polymer samples. In the case of sample P1-80, some of the diffraction peaks, at smaller angle 2θ, almost disappeared and this was accompanied by a significant decrease of the endothermic peak at 101°C on the DSC curve associated with the hard-segment melting, and by a distinct increase of the endothermic peak at 42°C, connected with the soft-segment melting.

The PURs based on PTMO-2000 (see Fig. 7) were less crystalline in comparison with the PCL-2000- and PTMO-1000-based ones. Their crystallinity degrees were small (except PUR P2-20) and they decreased as the soft-segment content in the polymer samples increased (see Table VIII). For sample P2-80, the WAXFIT program resolved a diffraction pattern (see Table VI) on two peaks with significantly high FWHM values (3.5° and 6.7°), and this points to the null crystallinity degree of this sample. The most distinct diffraction peaks were observed for sample P2-20 (see Fig. 10), which correlates with the high endothermic peak at 151°C on the DSC curve from the first heating scan (see Fig. 3). An increase in the PTMO-2000 content caused distinct changes on the XRD and DSC curves; the endothermic peak almost disappeared at ~ 100–150°C, but a higher endothermic peak appeared at ~ 0–20°C. The latter endothermic peak, originating from PTMO-2000, has no reflection in the XRD patterns received at room temperature. Thus, the crystallinity of this series of polymers (at room temperature) should only be connected with the crystallization of hard segments.

Hardness and tensile properties

Shore A/D hardness and tensile properties were determined for the PURs prepared at the molar ratio of NCO/OH = 1, and in the case of the PTMO-1000-based PURs also at 1.05, after pressing at 80 to 160°C under the pressure of ~ 10–30 MPa. Table IX and Figure 12 show the results of the investigations for the polymers.

Among the poly(ether urethane)s obtained from PTMO-1000 at the molar ratio of NCO/OH = 1 was brittle material and others with small (18–96%) elongation at break. Their tensile strengths were in the range of 6.2–15.2 MPa. The same polymers synthesized at the molar ratio of NCO/OH = 1.05 showed higher tensile strength (9.9–17.0 MPa) and elongation at break (17–436%), as well as higher hardness. Better mechanical properties of these PURs can be caused by their higher molecular weights, as is suggested by GPC data for PUR P1-60 and η_{red} values for all these PURs. The stress–strain curves of the PURs prepared at the molar ratio of NCO/OH = 1 and 1.05 are shown in Figure 12(A,B).

The poly(ether urethane)s with PTMO-2000 were characterized by higher tensile strength (9.7–23.5 MPa) and much higher elongation at break (57–

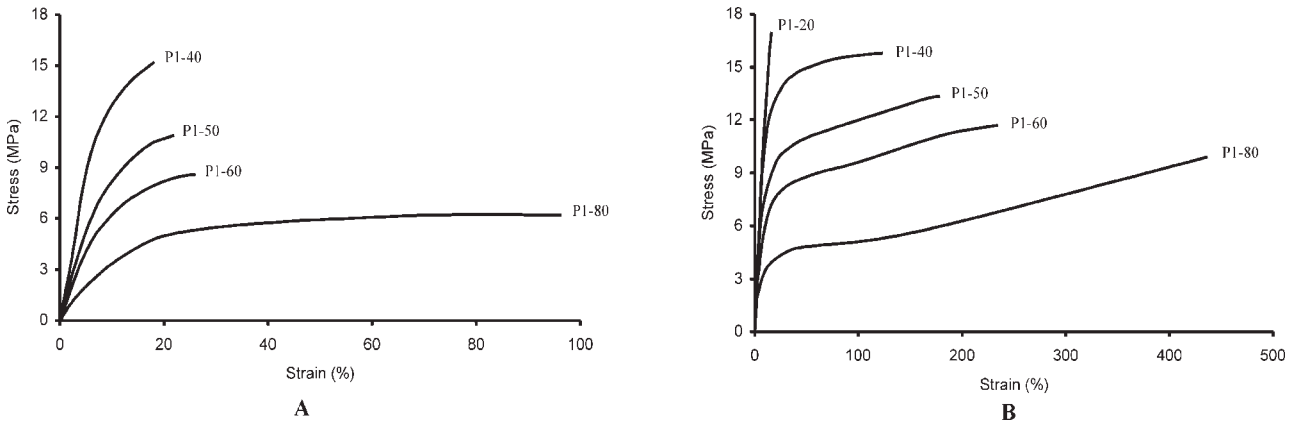

Figure 12 Stress–strain curves of the PURs obtained from PTMO-1000 at the molar ratio of NCO/OH = 1 (A) and 1.05 (B).

1953%) in comparison with the analogous ones with shorter polyether soft segment. These polymers also showed significantly lower modulus of elasticity and smaller hardness than the PURs from PTMO-1000.

In the case of the poly(ether urethane)s, as the PTMO content increased, hardness and the modulus of elasticity decreased, whereas elongation at break increased.

Generally, the PURs derived from PCL-2000 exhibited higher hardness and the modulus of elasticity, and smaller elongation at break in comparison with the corresponding poly(ether urethane)s with the same soft-segment length. In the case of these poly(ester urethane)s, as the PCL-2000 content increased, so did elongation at break. The increase in the soft-segment content first caused a decrease of both hardness and the modulus of elasticity, and then an increase of these parameters, which was higher for the modulus of elasticity. It was connected with the crystallinity originating from PCL-2000 (at room temperature) in samples L2-60 and L2-80, its content being higher.

Both in the series of PTMO-2000 and PCL-2000, polymers with the highest tensile strength (23.5 and 20.3 MPa, respectively) were obtained at 50 mol % soft-segment content.

CONCLUSIONS

In order to determine the effect of the molecular weight and structure of a soft segment on crystallinity and some properties of polymers, three series of novel thermoplastic segmented PURs were prepared from PTMO-1000, PTMO-2000, and PCL-2000, using the same hard segment EBTH/HDI. This effect was discussed in connection with the soft-segment content (20–80 mol %).

Most of the synthesized PURs possessed a partially crystalline structure (at room temperature), originating from hard and soft segments. In the case of the PURs with PTMO-2000, no crystallinity connected with soft segments was observed, because the T_m of soft segments was below room temperature. It was found that among the PURs with 20 mol % soft-segment content, the most crystalline turned out to be polymer P1-20 (with the highest hard-segment content), whereas the remaining two possessed similar crystallinity. On the other hand, among the PURs containing 40–80 mol % soft segments, crystallinity decreased in the following order of the polymer series: L2, P1, and P2. The resulting polymers (except PUR P1-20) were TPUs showing good low-temperature properties, with the poly(ether urethane)s showing lower T_gs (−75 to −61°C) than those shown by the poly(ester urethane)s (−54 to −52°C). In the case of the poly(ether urethane)s, lower T_gs and better microphase separation were exhibited by the PURs with longer soft segment PTMO-2000. Tensile strengths and elongation at break of the obtained TPUs were in the range of 6.2–23.5 MPa and 18–1953%, respectively. Comparing the TPUs synthesized at the molar ratio of NCO/OH = 1 it can be said that higher tensile strengths and higher elongations at break were achieved when longer soft segments (PTMO-2000 and PCL-2000) were used. Poly(ether urethane)s based on PTMO-1000 with better mechanical properties were obtained at the molar ratio of NCO/OH = 1.05. These polymers, prepared with excess of diisocyanate, showed greater tensile strengths and smaller elongations at break than the analogous materials described earlier,[47,48] synthesized from benzophenone-derivative or diphenylmethane-derivative chain extenders.

References

1. Randall D, Lee S, Eds. The Polyurethanes Book; Huntsman Polyurethanes: Everberg, Belgium, 2002.
2. Wirpsza, Z. Polyurethanes: Chemistry, Technology and Applications; Ellis Horwood: New York, 1993.
3. Hepburn, C. Polyurethane Elastomers; Applied Science: London, 1982.

4. Holden, G. In Kirk-Othmer Encyclopedia of Chemical Technology, 5th ed.; Kroschwitz, J.; Ed.; Wiley Interscience: New York, 2001; p 695.
5. Ulrich, H. In Encyclopedia of Polymers Science and Technology, 3rd ed.; Mark, H. F., Ed.; Wiley: New York, 2003; Vol. 4, p 26.
6. Gogolewski, S. Colloid Polym Sci 1989, 267, 757.
7. Rokicki, G.; Kowalczyk, T. Polymer 2000, 41, 9013.
8. Stokes, K.; McVenes, R.; Anderson, J. M. J Biomater Appl 1995, 9, 321.
9. Seefried, C. G., Jr.; Koleske, J. V.; Critchfield, F. E. J Appl Polym Sci 1975, 19, 2493.
10. Seefried, C. G., Jr.; Koleske, J. V.; Critchfield, F. E. J Appl Polym Sci 1975, 19, 2503.
11. Hesketh, T. R.; Van Bogart, J. W. C.; Cooper, S. L. Polym Eng Sci 1980, 20, 190.
12. Van Bogart, J. W. C.; Gibson, P. E.; Cooper, S. L. J Polym Sci Polym Phys Ed 1983, 21, 65.
13. Lorenz, R.; Els, M.; Haulena, F.; Schmitz, A.; Lorenz, O. Angew Makromol Chem 1990, 180, 51.
14. Szczepaniak, B.; Frisch, K. C.; Pęczek, P.; Mejsner, J.; Leszczyńska, I.; Rudnik, E. J Polym Sci Part A: Polym Chem 1993, 31, 3223.
15. Szczepaniak, B.; Frisch, K. C.; Pęczek, P.; Rudnik, E.; Cholińska, M. J Polym Sci Part A: Polym Chem 1993, 31, 3231.
16. Sun, S. J.; Hsu, K. Y.; Chang, T. C. J Polym Sci Part A: Polym Chem 1995, 33, 787.
17. Mix, R.; Goering, H.; Schultz, G.; Gründemann, E.; Gähde, J. J Polym Sci Part A: Polym Chem 1995, 33, 1523.
18. Mix, R.; Gähde, J.; Goering, H.; Schultz, G. J Polym Sci Part A: Polym Chem 1996, 34, 33.
19. Sun, S. J.; Chang, T. C. J Polym Sci Part A: Polym Chem 1996, 34, 771.
20. Lan, P. N.; Corneillie, S.; Schacht, E.; Davies, M.; Shard, A. Biomaterials 1996, 17, 2273.
21. Li, F.; Hou, J.; Zhu, W.; Hang, X.; Xu, M.; Luo, X.; Ma, D.; Kim, B. K. J Appl Polym Sci 1996, 62, 631.
22. Kim, B. K.; Lee, S. Y.; Xu, M. Polymer 1996, 37, 5781.
23. Martin, D. J.; Meijs, G. F.; Renwick, G. M.; Gunatillake, P. A.; McCarthy, S. J. J Appl Polym Sci 1996, 60, 557.
24. Martin, D. J.; Meijs, G. F.; Renwick, G. M.; McCarthy, S. J.; Gunatillake, P. A. J Appl Polym Sci 1996, 62, 1377.
25. Martin, D. J.; Meijs, G. F.; Gunatillake, P. A.; McCarthy, S. J.; Renwick, G. M. J Appl Polym Sci 1997, 64, 803.
26. Li, F.; Hang, X.; Hou, J.; Xu, M.; Luo, X.; Ma, D.; Kim, B. K. J Appl Polym Sci 1997, 64, 1511.
27. Lin, J. R.; Chen, L. W. J Appl Polym Sci 1998, 69, 1563.
28. Lin, J. R.; Chen, L. W. J Appl Polym Sci 1998, 69, 1575.
29. Martin, D. J.; Meijs, G. F.; Gunatillake, P. A.; Yozghatlian, S. P.; Renwick, G. M. J Appl Polym Sci 1999, 71, 937.
30. Kim, H. D.; Lee, T. J.; Huh, J. H.; Lee, D. J. J Appl Polym Sci 1999, 73, 345.
31. Chen, K. S.; Yu, T. L.; Tseng, Y. H. J Polym Sci Part A: Polym Chem 1999, 37, 2095.
32. Son, T. W.; Lee, D. W.; Lim, S. K. Polym J 1999, 31, 563.
33. Adhikari, R.; Gunatillake, P. A.; McCarthy, S. J.; Meijs, G. F. J Appl Polym Sci 2000, 78, 1071.
34. Jimenez, G.; Asai, S.; Shishido, A.; Sumita, M. Eur Polym Mater 2000, 36, 2039.
35. Bajsic, E. G.; Rek, V.; Sendijarevic, A.; Sendijarevic, V.; Frisch, K. C. J Elastomer Plast 2000, 32, 162.
36. Bajsic, E. G.; Rek, V. J Appl Polym Sci 2001, 79, 864.
37. Wen, T. C.; Fang, J. C.; Gopalan, A. J Appl Polym Sci 2001, 82, 1462.
38. Gorna, K.; Połowiński, S.; Gogolewski, S. J Polym Sci Part A: Polym Chem 2002, 40, 156.
39. Kloss, J.; Munaro, M.; De Souza, G. P.; Gulmine, J. V.; Wang, S. H.; Zawadzki, S.; Akcelrud, L. J Polym Sci Part A: Polym Chem 2002, 40, 4117.
40. Padmavathy, T.; Srinivasan, K. S. V. J Macromol Sci Part C: Polym Rev 2003, 43, 45.
41. Srinivasan, K. S. V.; Padmavathy, T. Macromol Symp 2003, 199, 277.
42. Bajsic, E. G.; Rek, V.; Agic, A. J Elastomer Plast 2003, 35, 311.
43. Wang, S. H.; Silva, L. F.; Kloss, J.; Munaro, M.; De Souza, G. P.; Wada, M. A.; Gomez, J. G. C.; Zawadzki, S.; Akcelrud, L. Macromol Symp 2003, 197, 255.
44. Prisacariu, C.; Buckley, C. P.; Caraculacu, A. A. Polymer 2005, 46, 3884.
45. Rogulska, M.; Podkościelny, W.; Kultys, A.; Pikus, S.; Poździk, E. Eur Polym Mater 2006, 42, 1786.
46. Rabiej, M.; Rabiej, S. Analiza krzywych dyfrakcyjnych polimerów za pomoc[ogon]a programu komputerowego WAXS-FIT. Poland, Bielsko-Biała: ATM; 2006.
47. Kultys, A.; Podkościelny, W.; Pikus, S. J Polym Sci Part A: Polym Chem 1999, 37, 4140.
48. Kultys, A.; Pikus, S. J Polym Sci Part A: Polym Chem 2001, 39, 1733.